

Durable Complete Response from Metastatic Melanoma after Transfer of Autologous T Cells Recognizing 10 Mutated Tumor Antigens

Todd D. Prickett¹, Jessica S. Crystal¹, Cyrille J. Cohen², Anna Pasetto¹, Maria R. Parkhurst¹, Jared J. Gartner¹, Xin Yao¹, Rong Wang³, Alena Gros¹, Yong F. Li¹, Mona El-Gamil¹, Kasia Trebska-McGowan¹, Steven A. Rosenberg¹, and Paul F. Robbins¹

Abstract

Immunotherapy treatment of patients with metastatic cancer has assumed a prominent role in the clinic. Durable complete response rates of 20% to 25% are achieved in patients with metastatic melanoma following adoptive cell transfer of T cells derived from metastatic lesions, responses that appear in some patients to be mediated by T cells that predominantly recognize mutated antigens. Here, we provide a detailed analysis of the reactivity of T cells administered to a patient with metastatic melanoma who exhibited a complete response for over 3 years after treatment. Over 4,000 nonsynonymous somatic mutations were identified by whole-exome sequence analysis of the patient's autologous normal and tumor cell DNA. Autologous B cells transfected with 720 mutated minigenes corresponding to the

most highly expressed tumor cell transcripts were then analyzed for their ability to stimulate the administered T cells. Autologous tumor-infiltrating lymphocytes recognized 10 distinct mutated gene products, but not the corresponding wild-type products, each of which was recognized in the context of one of three different MHC class I restriction elements expressed by the patient. Detailed clonal analysis revealed that 9 of the top 20 most prevalent clones present in the infused T cells, comprising approximately 24% of the total cells, recognized mutated antigens. Thus, we have identified and enriched mutation-reactive T cells and suggest that such analyses may lead to the development of more effective therapies for the treatment of patients with metastatic cancer. *Cancer Immunol Res*; 4(8); 669–78. ©2016 AACR.

Introduction

Immunotherapy has assumed a prominent role in the treatment of patients with metastatic cancer (1, 2). Complete durable tumor regressions have also been observed in 20% of melanoma patients receiving adoptive transfer of autologous tumor-infiltrating lymphocytes (TIL) that were expanded *in vitro* to cell numbers as high as 2×10^{11} T cells (3). Recent clinical trials that block interactions of inhibitory receptors such as CTLA-4 and PD-1 that are expressed on activated T cells have resulted in objective clinical responses in 30% to 40% of patients with melanoma (4), as well as 15% of patients with advanced squamous non-small cell lung cancer (5), and 43% of selected patients with metastatic urothelial bladder cancer (6). These observations indicate that T cells recognize antigens expressed by patients' tumors. Clinical responses to adoptive immunotherapy have been associated with the transfer of TILs that predominantly or exclusively recognize mutated

T-cell epitopes expressed by patient tumors (7–9). Direct evidence that T cells recognizing neoantigens may be important in tumor regression mediated by TILs is shown by the partial regression of a metastatic cholangiocarcinoma, still ongoing 20 months after transfer of a patient's autologous T cells that recognized a mutated class II-restricted ERBB2IP gene product (10). Observations made in patients receiving antibodies blocking the inhibitory molecules CTLA-4 (11) and PD-1 (12), as well as in mouse tumor models (13), suggest that checkpoint blockade responses may be associated with T-cell responses to mutated tumor antigens.

Extensive studies have focused on the identification of potential tumor rejection antigens in an attempt to derive principles that can guide future cancer immunotherapies. Toward this end, we evaluated the reactivity of T cells administered to a 54-year-old man with metastatic melanoma who exhibited a complete and durable regression of metastatic disease that is ongoing over 3 years after treatment. The approach used in these studies was based upon methods described in two recent studies from our laboratory indicating that mutated antigens recognized by patient TILs could be readily identified by whole-exome sequencing of autologous tumor samples (7, 9).

We identified dominant antigens recognized by a polyclonal population of *in vitro* expanded TILs. Whole-exome sequencing of the patient's tumor and normal cells was initially carried out to identify nonsynonymous somatic variants present in the patient's cancer. These variants were then aligned with those identified using RNA-Seq analysis of the same sample to generate a panel of candidate neoepitopes. Large-scale screening carried out with autologous B cells transfected with tandem minigene (TMG) constructs encoding candidate epitopes demonstrated that the

¹National Institutes of Health, National Cancer Institute, Surgery Branch, Bethesda, Maryland. ²Laboratory of Tumor Immunology and Immunotherapy, Bar-Ilan University, Ramat Gan, Israel. ³U.S. Food and Drug Administration, Bethesda, Maryland.

Note: Supplementary data for this article are available at Cancer Immunology Research Online (<http://cancerimmunolres.aacrjournals.org/>).

Corresponding Author: Todd D. Prickett, Center for Cancer Research, National Cancer Institute, 10 Center Drive, Building 10, Room 3W-3864, Bethesda, MD 20892. Phone: 301-496-8823; Fax: 301-339-3657; E-mail: prickettt@mail.nih.gov

doi: 10.1158/2326-6066.CIR-15-0215

©2016 American Association for Cancer Research.

bulk population of T cells used for patient treatment recognized 10 MHC class I–restricted neopeptides, but exhibited little or no recognition of the corresponding wild-type epitopes. The predominance of T cells that recognize the mutated epitopes in the population of administered T cells suggests that they may have played a significant role in mediating the long-term durable tumor regression seen in this patient, and provide support for continuing studies to identify and isolate T cells reactive with mutated epitopes for patient treatments.

Materials and Methods

Patient tissues and cell lines

Patient 3713 was a 54-year-old man with stage IV melanoma with multiple metastases to the lungs and lymph nodes (Fig. 1A and B). This patient underwent surgical resection of a metastatic lung lesion. TILs were grown from multiple tumor fragments, and Epstein-Barr virus (EBV)–transformed B cells were generated as described (14). In addition, a cell line was generated by culturing a fragment of the same metastatic lesion in 10% FBS and RPMI media. Selected TIL fragments were expanded *in vitro*, combined, and infused into the patient following a lymphodepleting regimen of nonmyeloablative chemotherapy plus 1,200 cGy of total body irradiation as described (NCI clinical trial NCT01319565). After receiving 6×10^{11} TILs and 4 doses of high-dose IL2, the patient experienced a complete durable tumor regression that is ongoing more than 3 years after treatment (Fig. 1C and D).

The autologous tumor cell line 3713 TC and 3713 EBV-transformed B cells were generated in house shortly after tumor resection (2013). HEK-293T and COS-7 cells were purchased from the American Type Culture Collection in 2008 and cultured in RPMI-1640 (Life Technologies) media supplemented with 5% FBS, neither cell line has been authenticated recently. Patient TILs were maintained in media consisting of equal volumes of RPMI-1640 and AIM V media (Life Technologies) supplemented with 5% human serum and 3,000 IU of IL2. Coculture assays performed in 96-well U-bottom plates at a 1:1 ratio of T cells to target cells in 200 μ L of 1:1 RPMI-1640:AIM V media supplemented with 5% human serum for 16 to 20 hours were screened for IFN γ levels in the supernatant via ELISA as previously described (15).

Normal B cells were generated from autologous peripheral blood mononuclear cells (PBMC) as described (16).

Whole-exome sequencing and RNA-Seq analysis

Genomic DNA purification, library construction, exome capture of approximately 20,000 coding genes, and next-generation sequencing of 3713 fresh tumor (FrTu) embedded in optimal cutting temperature (OCT; Sakura Finetek) and a matched normal pheresis sample were performed at Personal Genome Diagnostics as previously described (17). In addition, a whole-exome library was prepared using Agilent Technologies SureSelectXT Target Enrichment System for paired-end libraries and subsequently sequenced on a NextSeq 500 desktop sequencer (Illumina). The library was prepped using gDNA (3 μ g) isolated from the ten 10- μ m OCT sections following the manufacturer's protocol (Agilent Technologies). Paired-end sequencing was done with an Illumina mid-output flow cell kit (300 cycles). An mRNA sequencing library was prepared from the autologous 3713 tissue culture (TC) line using an Illumina TruSeq RNA library prep kit following the manufacturer's protocol. RNA-Seq libraries were paired-end sequenced on a HiSeq 2000 sequencer (Illumina) for 100 cycles at the FDA sequencing core laboratory.

Nonsynonymous somatic variants were identified from whole-exome sequencing of 3713 FrTu using filters consisting of a minimum of three variant reads, an 8% variant allele frequency (VAF), less than or equal to a 1% VAF in normal DNA, and absence in the set of SNPs in the 1000 Genomes SNP database or presence in the database at a VAF of less than 1%. Approximately 83% of the single or dinucleotide substitutions represented C-to-T transitions (Supplementary Fig. S1), the common signature for mutations induced by ultraviolet light (18). Further analysis revealed that approximately 1,000 variants were derived from transcripts with expression (expressed as fragments per kilobase per million transcripts or FPKM) between the range of 1 and 900 FPKM units. In an attempt to screen targets expressed to various degrees, but also to limit screening to gene products that were more likely to be recognized by T cells, the top 720 variants, corresponding to a FPKM value of approximately 3 or higher, were chosen for further evaluation (Supplementary Table S1). After annotation, mutated

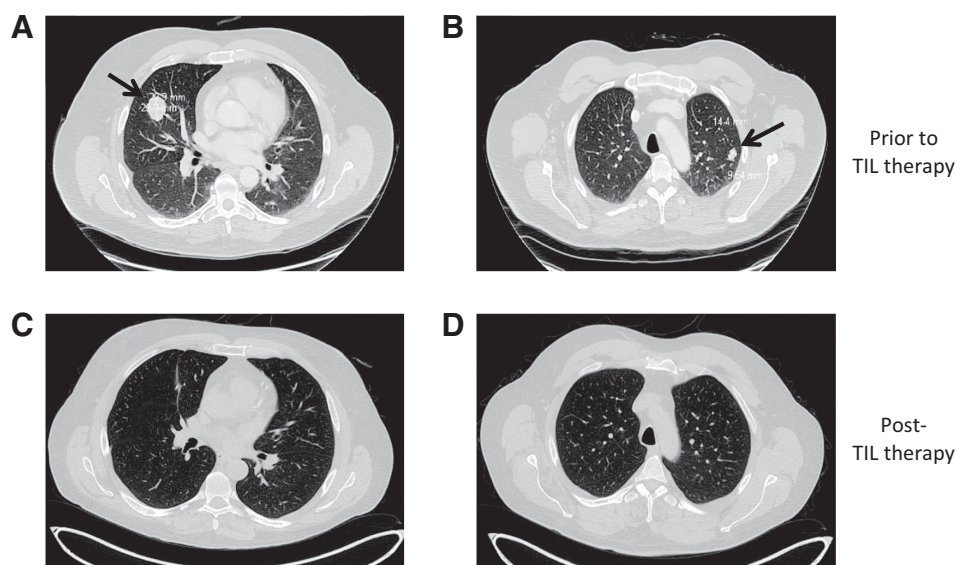


Figure 1.

Clinical response of patient 3713 after treatment with adoptive cell therapy. CT scans show the disease present in both lobes of the lung (A and B) prior to surgical resection and TIL therapy (C and D). The 3-cm lesion in the left lobe (A) was resected and used to derive patient-specific TILs. D shows patient's lungs clear of disease. Black arrows in A and B show areas of metastatic disease.

transcripts were extracted from the NCBI Reference Sequence, UCSC Known Gene and ENSEMBL databases, and in the case of single-nucleotide variants, peptide sequences encompassing the mutated codon plus the 12 flanking amino acids, except in cases in which derived mutations were present within the first or final 12 amino acids of the protein transcript. For the two frameshift deletions that were identified, the 12 amino acids prior to the deletions were extracted, and sequences beyond the mutation site were translated until the first stop codon was encountered. For the single stop-loss variant that was identified, the 12 amino acids prior to the mutated stop codon were translated, along with downstream coding sequences prior to the first stop codon.

TMG library construction

Candidate-mutated peptide sequences were reverse-translated and codon optimized using online tools available at Life Technologies and IDT DNA, Inc. Of the 720 variants chosen for evaluation, 718 contained either a single or a dinucleotide nonsynonymous mutation, one contained a frameshift deletion of a single nucleotide and one contained a mutation resulting in the loss of a stop codon. In addition, for 10 of the nonsynonymous mutations, alternatively spliced gene products that gave rise to two peptide sequences differing in regions flanking the mutation site were evaluated. Transcripts were grouped into TMGs encoding between 10 and 12 individual minigenes, with no amino-acid spacers between individual minigenes. A total of 62 TMG constructs were then synthesized (Invitrogen) and cloned into a modified pcDNA3.1 expression vector (Invitrogen). The TMGs were inserted downstream of, and in-frame with, sequences encoding an adenovirus E19 signal-peptide sequence (19) and upstream of, and in-frame with, a LAMP1 endosomal targeting sequence (20), using the In-Fusion Advantage PCR cloning Kit (Clontech) according to the manufacturer's instructions.

The TMG constructs were linearized by digestion with the NsiI restriction enzyme for 16 hours at 37°C followed by phenol:chloroform:isoamyl alcohol (25:24:1) extraction and ethanol precipitation, and *in vitro* transcription performed using a T7 IVT kit (Life Technologies) with linear DNA (1 µg) for 2 hours at 37°C followed by 15-minute DNaseI treatment, and mRNA was purified using the Qiagen QIAeasy RNA extraction/clean-up Kit (Qiagen) per the manufacturer's protocol. Autologous B cells transformed with EBV were then electroporated as described (9) with 1 to 2 µg of the *in vitro*-transcribed RNA followed by incubation for 16 to 20 hours at 37°C. Autologous TIL 3713 (100,000 cells) were cocultured with an equal number of transfected EBV cells in 96-well plates overnight at 37°C, with cocultures of 3713 TC cells with autologous TILs serving as a positive control. The IFN γ released in coculture supernatants was measured with an ELISA assay.

Screening assay and identification of mutated epitopes recognized by TIL 3713

TMGs that stimulated at least 200 pg/mL of IFN γ and for which the resulting IFN γ concentration was at least twice that of control cocultures (EBV-transformed B cells transfected with the irrelevant green fluorescent protein) were further evaluated. Constructs that encoded the wild-type version of individual minigenes or that had between one and six of the minigenes present in the original TMGs deleted were generated for screening. Mutated candidates that failed to stimulate significant cytokine release from TIL 3713

when deleted or reverted back to wild-type sequences were presumed to encode mutated T-cell epitopes.

To identify the MHC class I restriction elements that presented the mutated epitopes, HEK-293T cells were cotransfected with plasmid DNA corresponding to individual positive TMGs and individual constructs encoding each of the six MHC class I restriction elements expressed by the patient's normal and tumor cells (HLA-A*02:01, A*29:02, B*44:03, B*51:01, C*15:02, or C*16:01). The Immune Epitope Database (IEDB) NetMHC consensus-binding algorithm (21) was used to identify candidate minimal epitopes and synthesized as crude peptides (Peptide 2.0), pulsed on 3713 EBV B cells, and evaluated for their ability to stimulate significant cytokine release from TIL 3713.

Peptides were picked based on both the IC₅₀ and percentile rank with a cutoff of ≤ 500 nmol/L and 3.0, respectively. Peptides with an RPKM (reads per kilobase of transcript per million mapped reads) ranging from 3 to several hundred (determined from RNA-Seq analysis) were coupled to NetMHC IC₅₀ and percentile rank to define which peptides to screen. Positive peptides and the corresponding wild-type peptides were synthesized, high-performance liquid chromatography (HPLC)-purified, and $\geq 95\%$ purity (Peptide 2.0). Autologous EBV-transformed B cells were then pulsed with varying concentrations of the putative minimal epitopes for 2 hours at 37°C, washed once, and evaluated in IFN γ -release assays.

T-cell receptor analysis

The frequencies of individual T-cell clonotypes were determined by T-cell receptor (TCR) analysis of bulk PBMC obtained before and after adoptive transfer of bulk infusion TILs, and of CD8⁺, CD8⁺PD-1⁺, and CD8⁺PD-1⁻ T cells that were electronically sorted from a 3713 FrTu digest as described (22). Cell pellets were snap frozen and sent to Adaptive Biotechnologies for genomic DNA extraction and ImmunoSEQ TCR β survey sequencing. TCR α - and β -chain sequences were identified by amplifying sequences using a 5'RACE protocol as described (23) from T cells that were cloned by limiting dilution from TIL 3713 or from T cells that were sorted based upon upregulation of 4-1BB expression following stimulation with cells pulsed with mutated epitopes (24). Functional TCRs were generated by synthesizing constructs encoding α -chain sequences joined to β -chain sequences with a self-cleaving picornavirus P2A sequence (25) in the pMSGV1 retroviral vector, and activity was assessed by coculturing TCR-transduced PBMCs with tumor or peptide-pulsed target cells, as described (26). Isolation of CD8⁺ T cells from PBMCs was carried out using a CD8 T-cell enrichment kit (BD Biosciences).

Results

Whole-exome sequencing of fresh uncultured tumor and normal cells from patient 3713 initially indicated that this tumor contained over 4,000 nonsynonymous somatic variants, a relatively high mutational load in comparison with the majority of cutaneous melanomas (27), although melanomas that possess similar or higher mutation rates have been identified in previous studies (28, 29). Expression of the corresponding mutated transcripts was evaluated by RNA-Seq analysis of a TC cell line generated from 3713, FrTu, from which 720 of the most highly expressed mutated gene products were further evaluated.

Sixty-two TMGs, encoding the selected variants plus the 12 upstream and downstream flanking residues were constructed,

and autologous EBV B cells were transfected with *in vitro* transcribed RNA from these constructs. The autologous TIL 3713 cells used to treat the patient were >98% CD8⁺ (data not shown) and recognized targets transfected with TMGs 2, 5, 6, 9, 17, 20, 23, 32, 39, and 60 (Fig. 2A).

Initially, we synthesized and tested candidate high-affinity HLA A*02:01-binding peptides, identified from the mutated transcripts using an algorithm designed to predict binding to MHC class I gene products (21), for recognition by TIL 3713. TIL 3713 cells recognized a mutated SRPX peptide encoded by TMG-2 and a mutated WDR46 peptide encoded by TMG-9 (Table 1; ref. 30).

To identify other mutated antigens recognized by TIL 3713 T cells, individual minigenes were either reverted back to wild-type sequences or deleted from the TMG constructs. Reversion of individual sequences within the TMGs to the appropriate wild-type sequences led to the identification of TPX2, PRDX3, SEC22C, and CENPL as the antigens targeted in TMG-5, 6, 17, and 60, respectively, whereas evaluation of truncated TMGs led to the identification of HELZ2, GCN1L1, AFMID, and PLSCR4 as the

antigens targeted in TMGs 20, 23, 32, and 39, respectively (data not shown). None of the 10 mutated genes identified as targets of TIL 3713, which are briefly described in the Supplementary Text, have been implicated as cancer genes. Genes that are mutated in a relatively small proportion of individual tumors, however, may play a role in tumor development (31). It is notable that identical mutations in the HELZ and TPX2 genes have been observed in additional tumors (see Supplementary Text).

The HLA restriction element involved with presentation of the eight additional mutated antigens recognized by TIL 3713 was then identified by cotransfecting HEK-293T and COS7 cells with the individual TMGs identified in the initial screening assays in combination with each of the six individual MHC class I alleles expressed by patient 3713. The results of cocultures with transfected HEK-293T cells confirmed that TIL 3713 recognized SRPX in the context of HLA-A*02:01 (Fig. 2B). Targets transfected with TPX2 and SEC22C were recognized in the context of HLA-B*44:03, whereas targets transfected with PRDX3, HELZ2, GCN1L1, AFMID, PLSCR4, and CENPL were recognized in the

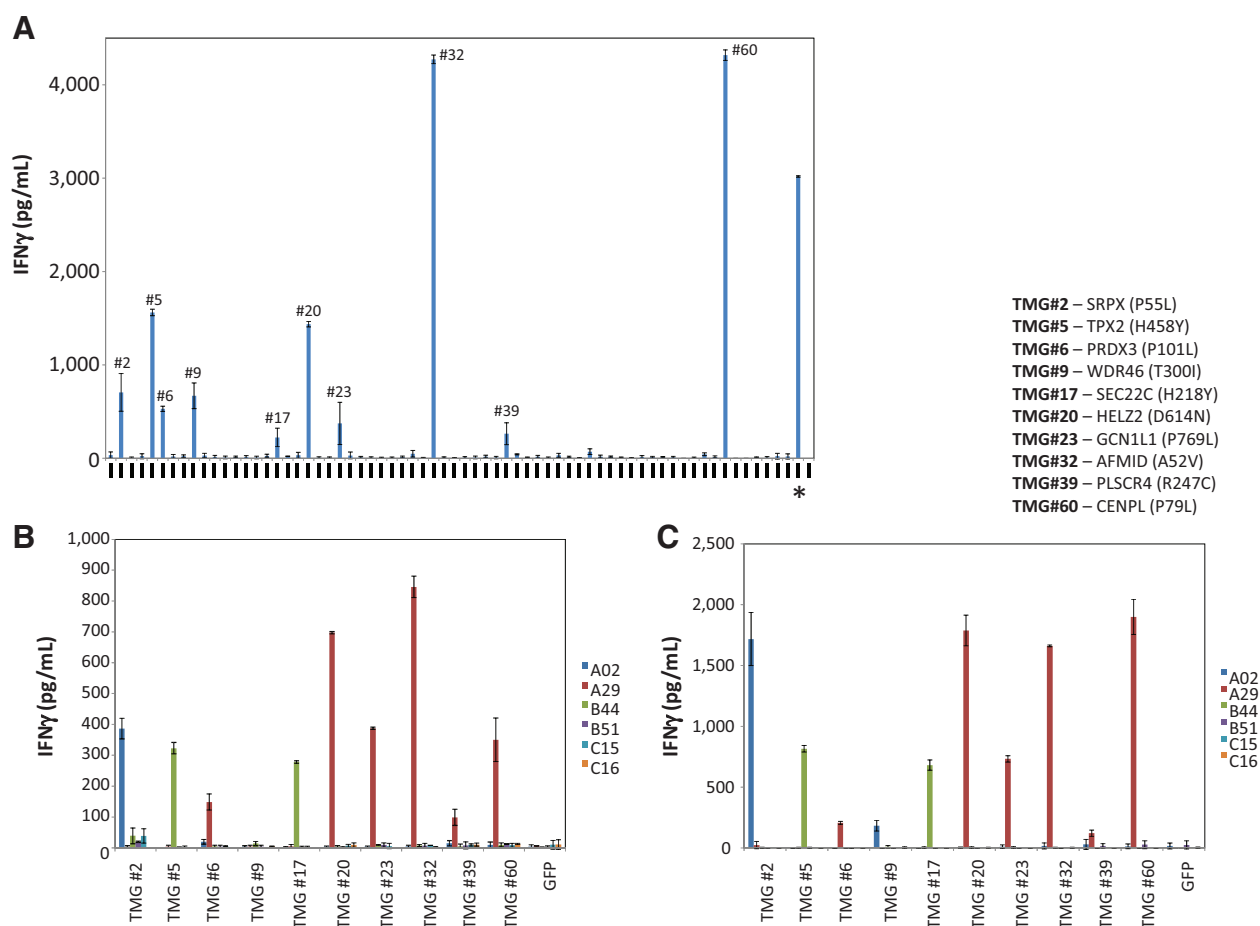


Figure 2.

Screening of patient 3713 autologous infusion bag TILs for reactivity to TMGs. **A**, autologous B cells transformed with EBV were transfected with IVT RNA from TMG-1 to TMG-62 individually and then cocultured with autologous infusion bag TIL. IVT RNA expressing GFP was a negative control, and autologous TIL 3713 mel cell line (*) was used as positive control. **B**, HEK-293T cells were transiently cotransfected with positive patient 3713 TMGs in the presence of patient-specific HLAs (A*020101, A*290201, B*440301, B*510101, C*150101, or C*160101). GFP expression construct was used as a negative control. **C**, COS7 cells were transiently cotransfected with positive patient 3713 TMGs in the presence of patient-specific HLAs (A*020101, A*290201, B*440301, B*510101, C*150101, or C*160101). GFP expression construct was used as a negative control.

Table 1. Mutated antigens recognized by TIL 3713

Gene	Transcript ID	Chromosome: position	Amino-acid change	cDNA change	Mutated amino-acid sequence	Wild-type amino-acid sequence	HLA restriction element	Mutant IC ₅₀ (nmol/L)	Mutant rank	Wild-type IC ₅₀ (nmol/L)	Wild-type rank	RPKM
SRPX	uc004ddy.2	chrX:38033598	P55L	C164T	TLWCSPKIV	TPWCSPKIV	A*02:01	12	0.6	12,683	18	133
WDR46	uc003ods.3	chr6:33254984	T300I	C899T	FLIYLDVSV	FLTYLDVSV	A*02:01	5	0.3	8	0.4	40
PRDX3	uc001lec.3	chr10:120933972	P101L	C302T	FFYLLDFTF	FFYPLDFTF	A*29:02	16	0.4	7	0.3	49
HELZ2	uc002yfm.2	chr20:62198871	D614N	G1840A	QTNPVTLQY	QTD [~] PVTLQY	A*29:02	18	0.4	144	1.2	20
GCN1L1	uc001txo.3	chr12:120599720	P769L	C2306T	IMQTLAGELY	IMQTPAGELY	A*29:02	43	0.4	49	0.4	18
AFMID	uc002juz.3	chr17:76198784	A52V	C155T	EVL [~] PFFLFF	EALPFFLFF	A*29:02	156	1.2	1,003	2.8	11
PLSCR4	uc010huz.3	chr3:145914466	R247C	C739T	R [~] VCGPCSTY	RVRGPCSTY	A*29:02	247	1.6	586	2.2	9
CENPL	uc001gje.4	chr1:173776589	P79L	C236T	TL [~] YSLTLLY	TL [~] YSLTPLY	A*29:02	2	0.1	3	0.2	4
TPX2	uc010gdv.1	chr20:30371683	H458Y	C1480T	TEDEHF [~] FEFY	TEDEHF [~] FEFH	B*44:03	153	0.5	9,325	4.4	55
SEC22C	uc003clj.3	chr3:42597481	H218Y	C652T	AEHSLQV [~] AY	AEHSLQV [~] AH	B*44:03	13	0.2	589	1.1	23

context of HLA-A*29:02 (Fig. 2B). Similar results were observed using COS7 cells transfected with TMGs 2, 5, 6, 17, 20, 23, 32, 39, and 60, but in addition, TIL 3713 recognized COS7 cells transfected with WDR46 in the context of HLA-A*02:01. Responses against COS7 transfectants were generally more robust than responses to HEK-293T transfectants, which may have been responsible for the finding that TIL 3713 recognized COS7 but not HEK-293T cells that were cotransfected with TMG-9 and HLA-A*02:01 (Fig. 2B and C).

The minimal peptide epitopes from each of the positive mutated gene products predicted to bind with the highest avidity to the appropriate class I MHC alleles were then identified using the consensus IEDB peptide/MHC binding algorithm (Table 1; ref. 29) and synthesized to evaluate their recognition by TIL 3713. Candidate epitopes within the 25 amino-acid sequences encoded in TMGs that were predicted to possess binding affinities of ≤ 500 nmol/L or to be within the top 2% of predicted binders to the appropriate HLA class I alleles identified as restriction elements (HLA-A*02:01, HLA-A*29:02, and HLA-B*44:03) for the 10 neoepitopes were then synthesized and evaluated for recognition by TIL 3713. HLA class I (B*51:01, C*15:02, and C*16:01) alleles were not screened for binding via the IEDB NetMHC prediction algorithms due to lack of recognition in the coexpression/coculture experiment. Minimal epitopes of either 9 or 10 amino acids, predicted to bind the appropriate HLA class I alleles, were identified for each of the 10 neoantigens recognized by TIL 3713 (Fig. 3). The corresponding wild-type peptides elicited little or no response from the TIL, indicating that the T cells specifically recognized the altered residues in each of the positive peptides (Fig. 3). The minimal concentrations of the mutant peptides required to stimulate significant cytokine release from TIL 3713 ranged between 0.1 and 1.0 ng/mL for the HLA-A*02:01 and A*29:02 restricted epitopes, whereas higher concentrations of the two epitopes recognized in the context of HLA-B*44:03, SEC22C, and TPX2 peptides were required to stimulate significant cytokine release from TIL 3713 (Fig. 3). Residues altered in the SRPX, HELZ2, AFMID, TPX2, and SEC22C peptides were predicted to enhance peptide binding affinity by a factor of between 6- and 1,000-fold to the appropriate MHC alleles, whereas changes in the WDR46, GCN1L1, PLSCR4, and CENPL peptides were predicted to result in a less than 3-fold enhancement in binding affinity to the appropriate alleles (Table 1). The change in the PRDX3 epitope was predicted to result in an approximately 2-fold decrease in binding HLA-A*29:02; nevertheless, the mutated peptide was predicted to bind to this MHC allele with a relatively high affinity (16 nmol/L).

We then evaluated the TCR clonotypes within the autologous 3713 TC line that recognized mutated tumor epitopes. We isolated mutation-reactive TCRs from these clones or from CD137⁺ T cells that had been FACS sorted from IB TIL 3713 after stimulation with mutated TMGs (Table 2 and Fig. 4). Deep sequencing of TCR V β regions revealed that the top 20 clonotypes in the infused TILs ranged in frequencies between 4.5% and 1.3% (Table 2). Analysis of T-cell clones and T cells transduced with TCR α and β pairs isolated from antigen-reactive T cells revealed that 9 of the top 20 clonotypes recognized an individual epitope derived from either the CENPL, SRPX, AFMID, HELZ2, or SEC22 mutated transcripts (Table 2 and Fig. 4A–F). Screening of limiting-dilution clones or T cells that upregulated 4-1BB in response to antigen stimulation did not lead to the isolation of the T cells corresponding to the remaining 11 clonotypes, for which the reactivities remain unknown. The T cells that recognized the mutated CENPL, SRPX, HELZ2, and SEC22 epitopes also recognized autologous 3713 TC cells, whereas AFMID-reactive T cells showed little or no recognition of 3713 TC (Fig. 4). Five of the top 7 clonotypes recognized the mutated SRPX epitope at frequencies ranging between approximately 2% and 4% of the infused TILs, and single clonotypes recognizing the mutated CENPL, HELZ2, SEC22C, and AFMID epitopes each represented between 1% and 2% of the infused TILs (Table 2 and Fig. 4C–E). Approximately 12% of the infused TIL 3713 were reactive with an HLA-A*02:01 tetramer prepared with the mutated SRPX peptide (30), which was comparable with the total frequency of the 5 dominant SRPX-reactive clonotypes detected in IB TIL 3713 (14%). The factors responsible for the predominant reactivity of IB TIL 3713 against the mutated SRPX epitope are unknown. One possibility could be the relatively high expression of this gene product (Supplementary Table S1). The 5 dominant SRPX-reactive clonotypes detected in the infused TILs also represented the 5 most dominant T-cell clonotypes in the peripheral blood 5 weeks after adoptive transfer, each of which appeared to be represented in the peripheral blood at levels that were similar or somewhat higher than those observed in the infused TILs (Table 2). Four of the 5 SRPX-reactive clonotypes were also detected approximately 1 year after transfer at levels that ranged between 1% and 1.9% of peripheral T cells, and clonotypes reactive with the CENPL, HELZ2, and SEC22C epitopes represented 1.2, 1.0, and 0.5%, respectively, of peripheral T cells at this time (Table 2). T-cell clonotypes reactive with the mutated CENPL, SRPX, HELZ2, SEC22, and AFMID epitopes were represented in the 100 most

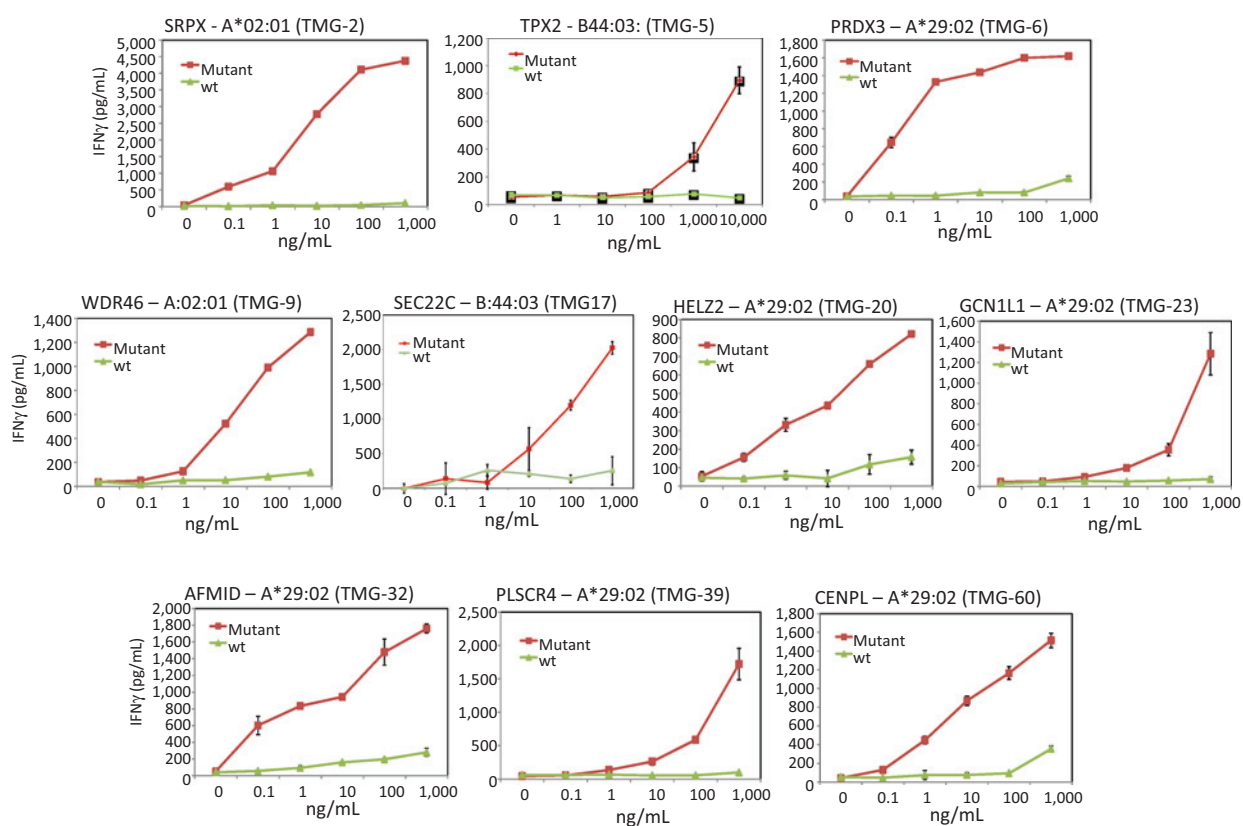


Figure 3.

Minimal neopeptide dose curve analysis with pulsed EBV cocultured with autologous TIL. EBV cells were pulsed with between 1,000 and 0.1 ng/mL of mutant or wild-type HPLC-purified peptides with the exception of TPX2 peptides, which were pulsed at concentrations ranging between 10,000 and 1 ng/mL, and the release of IFN γ following an overnight culture with TIL 3713 was determined. Each neopeptide dose-response curve was run three independent times. The gene names, HLA restriction elements, and TMG constructs encoding the mutated epitopes are shown above each graph.

frequent clonotypes detected in a population of CD8⁺PD-1⁺ T cells sorted from a FrTu digest at levels that were between 3-fold and more than 200-fold higher than in the corresponding CD8⁺PD-1⁻ population (Table 2), as demonstrated in a recent study evaluating the reactivity of T cells isolated from a panel of melanoma FrTu samples (21). None of the remaining clonotypes were evaluated due to our inability to identify T-cell clones or appropriate TCR α/β pairs, with the exception of the eighth and ninth clonotypes. For these clonotypes, TCRs were constructed with α - and β -chain sequences identified using the single-cell PCR approach; however, the resultant TCRs did not recognize the autologous 3713 TC line (data not shown). These results provide support for the hypothesis that T cells recognizing tumor-specific mutations can play a dominant role in the ongoing complete tumor regressions seen in some patients following the adoptive transfer of autologous tumor-reactive T cells.

Discussion

Antigens recognized by tumor-reactive T cells isolated from cancer patients can be categorized into four broad groups that include differentiation antigens that possess a limited distribution in normal tissues, normal self-antigens that are highly

overexpressed in tumor cells, cancer-germline antigens for which expression is limited to germ cells, and mutated antigens. The role of T cells targeting specific tumor antigens in control or regression of metastatic lesions, however, is unclear.

Regressions of multiple metastatic lesions were observed in patients with melanoma who received autologous T cells transduced with TCRs recognizing the melanocyte differentiation antigens MART-1 and gp100 (32). Responses, however, were often of short duration and severe dose-limiting toxicity, presumably resulting from the expression of these antigens in normal melanocytes. Durable complete tumor regressions were observed in 3 of 20 melanoma and 1 of 18 synovial cell sarcoma patients who received autologous T cells directed to the cancer-germline antigen NY-ESO-1 (33). However, most common cancers express little of this antigen, which limits its usefulness therapeutically. Although 1 of 9 patients who received T cells directed to a MAGE-A3 epitope had a long-term complete response, 3 patients experienced unexpected severe neurologic toxicity (34).

The durable complete regressions observed in about 20% of melanoma patients receiving oligoclonal populations of autologous TILs (3) were not associated with normal tissue toxicity, indicating that clinical responses can be mediated by T cells recognizing antigens with limited or no expression in normal tissues. Many long-term complete responses to TILs in melanoma

Table 2. Sequence and reactivity of dominant T-cell clonotypes in TIL 3713

Rank ^a	Infused TILs		CDR3b aa sequence	Autologous tumor reactivity	Clone/TRA, TRB pair	Antigen reactivity	Pre-PBMC		PD-1 ⁻ /PD-1 ⁺ CD8 ⁺ T cells (FrTu)		Post 1 month		Post 1 year	
	Frequency (%)	TR-BV					Rank	Frequency (%)	Rank	Frequency (%)	Rank	Frequency (%)	Rank	Frequency (%)
1	4.5	15-1	ATGTGGNDYEQYF	Yes	TCR T4 ^b	CENPL	52,466	0.0005	19/481	1.0/0.05	7	2.8	8	1.2
2	3.9	5-6	ASSLDRKKAFF	Yes	TCR MP-1	SRPX	ND ^c	<0.0001	86/ND	0.24/<0.001	1	4.5	4	1.9
3	3.5	28-1	ASSGKDRPHEQYV	NT ^d	Not identified	—	ND	<0.0001	220/ND	0.05/<0.001	19	1.1	23	0.7
4	2.8	11-1	ASSLIQVGYEQYF	Yes	Clone XY-51	SRPX	49,395	0.0005	22/591	0.91/0.04	2	4.5	ND	<0.0003
5	2.6	5-6	ASSLGPVYEQYF	Yes	Clone XY-6	SRPX	ND	<0.0001	10/198	1.6/0.01	3	4.3	6	1.6
6	2.6	10-2	ASGGAITDTQYF	Yes	Clone XY-3	SRPX	27,655	0.0012	3/963	3.2/0.02	4	4.1	7	1.4
7	2.5	10-2	ASSEGHFSGNTIYF	Yes	Clone XY-38	SRPX	ND	<0.0001	38/450	0.55/0.05	5	4.1	14	1.00
8	2.1	4-3	ASSQDDSGAKNIQYF	No	TCR 8	—	45,870	0.0006	507/1419	0.02/0.008	6	3.4	17	0.9
9	2.0	4-1	ASSQGLPQPHF	No	TCR 9	—	ND	<0.0001	39/60	0.54/0.22	10	1.8	18	0.8
10	1.8	27-1	ASSLNSGHTQYF	Yes	TCR T8-1	HELZ2	15,120	0.0017	2/112	6.5/0.15	9	2.2	12	1.0
11	1.7	28-1	ASSPGPGLTYEQYV	NT	Not identified	—	ND	<0.0001	80/1291	0.26/0.012	15	1.4	140	0.09
12	1.7	28-1	ASSLHGSSSYEQYV	NT	Not identified	—	21,157	0.0014	307/305	0.70/0.071	21	0.9	59	0.3
13	1.6	29-1	SVEDRRGPFYGYTF	Yes	Clone XY52	SEC22C	ND	<0.0001	41/910	0.53/0.024	17	1.3	28	0.5
14	1.6	5-5	ASSLAQPNPQPHF	NT	Not identified	—	44,967	0.0007	35/40	0.56/0.33	8	2.7	9	1.2
15	1.6	14-1	ASSQYAVRVGDTEAFF	NT	Not identified	—	ND	<0.0001	8/507	2.0/0.046	59	0.3	44	0.3
16	1.5	13-1	ASSSGLAGEQFF	NT	Not identified	—	ND	<0.0001	211/ND	0.056/<0.001	14	1.7	30	0.5
17	1.5	5-4	ASSLLTEAFF	NT	Not identified	—	5,839	0.0027	1/268	9.7/0.079	22	0.9	62	0.3
18	1.4	7-9	ASSHQAGALYNEQFF	Yes	TCR HI-2	AFMID	ND	<0.0001	94/262	0.20/0.079	41	0.5	56	0.3
19	1.3	12	ASGPRSEQFF	NT	Not identified	—	ND	<0.0001	529/ND	0.012/<0.001	50	0.4	48	0.3
20	1.3	25-1	ASLERGVSTDTQYF	NT	Not identified	—	ND	<0.0001	ND/ND	<0.001/<0.001	27	0.7	29	0.5

^aThe rearranged TR-BV region sequences of the indicated T-cell populations were analyzed by deep-sequencing, nucleotide sequences present at two or more copies were ranked from the highest to the lowest frequency, and amino-acid sequences of the CDR3 regions were determined, as described in Materials and Methods.

^bAnalysis of reactivity of T-cell clones and the TCRs is presented in Fig. 4. "Not identified" indicates that T cells expressing this TR-BV sequence could not be evaluated because a clone was not isolated and the appropriate TRAV sequence expressed by this clonotype could not be identified.

^cND, not detected within the limits of the assay [0.0001% for pre-PBMC, 0.001% for PD-1⁺ and PD-1⁻ CD8⁺ T cells (FrTu), 0.0004% for post 1 month, and 0.0003% for post 1 year samples].

^dNT, not tested.

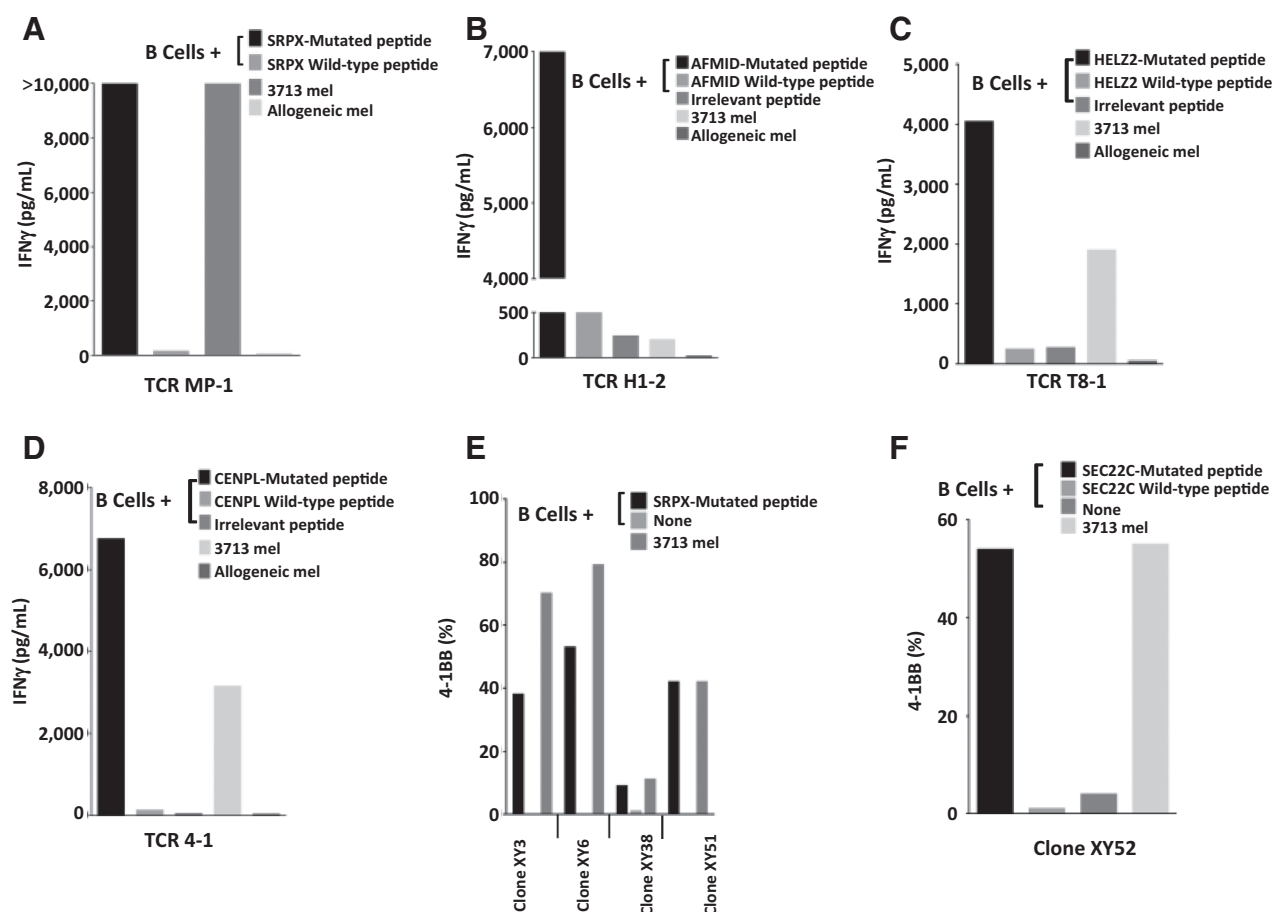


Figure 4.

Reactivity of clones or TCRs corresponding to predominant clonotypes in TIL 3713. Responses of allogeneic whole PBMCs (A–C) or CD8-enriched T cells (D) transduced with TCRs reactive with the mutated SRPX (A), AFMID (B), HELZ2 (C), or CENPL epitopes were evaluated by measuring the release of IFN γ in response to T2 cells (A) or autologous EBV B cells (B–D) pulsed with the appropriate peptides. Transduced T cells were also evaluated for their ability to release IFN γ in response to either the autologous TC line or an allogeneic melanoma TC line. In addition, T-cell clones isolated from TILs that were reactive with the mutated SRPX epitope (E) or the mutated SEC22C epitope (F) were evaluated for their ability to upregulate 4-1BB in response to autologous normal B cells (E) or EBV B cell (F) targets pulsed with the appropriate peptides or the autologous TC line (graphs represent two independent experimental repeats).

did not involve recognition of shared nonmutated antigens but, rather, contained dominant populations of T cells recognizing patient-specific neoantigens (7, 9, 35, 36). The melanomas evaluated in these studies contained between approximately 250 and 3,000 somatic nonsynonymous mutations (7, 9, 35, 36; S.A. Rosenberg, unpublished data), suggesting no direct association between the response to adoptive immunotherapy and mutation rate, a conclusion further supported by ongoing durable objective response that was observed in a patient with cholangiocarcinoma following the adoptive transfer of a highly enriched population of autologous CD4⁺ T cells reactive with a mutated ERBB2IP protein expressed by autologous cholangiocarcinoma tumor cells possessing only 26 nonsynonymous somatic mutations (10) and in a melanoma patient with only 70 nonsynonymous somatic mutations (9). The effects of mutations that give rise to neoepitopes, combined with intrinsic features of tumor antigen-reactive T cells—avidity, differentiation state, and proliferative potential (22, 37)—all influence responses to immunotherapy. These factors

are likely, for the most part, to be independent of the number of neoepitope targets expressed by patients' tumors.

T cells recognizing neoantigens probably play a role in clinical responses to immune checkpoint inhibitors. In one report, clinical responses in patients with metastatic melanoma to ipilimumab or tremelimumab, antibodies directed against the inhibitory protein CTLA-4, were associated with the number of nonsynonymous somatic mutations detected in those cancers (11). Translation of the sequences surrounding the nonsynonymous mutations led to the identification of a 4-amino-acid motif, termed a neoantigen signature, which was associated with clinical response to anti-CTLA-4 therapy, although this finding has not been confirmed in additional studies. In a second study, clinical responses of patients with non-small cell lung cancer to administration of pembrolizumab, an antibody directed toward the immune checkpoint inhibitor PD-1, were associated with mutational burden, and treatment was associated with the peripheral expansion of T cells reactive with a neoantigen target in one of the patients (12).

Here, we identified 10 distinct mutated T-cell epitopes as targets of the autologous TILs out of the 720 nonsynonymous somatic mutations with the highest transcript expression in the 3713 tumor. Between 1 and 5 of the 20 most frequent T-cell clonotypes present within the infused T-cell population, which ranged in frequency between 4.5% and 1.4% of total T cells, recognized the mutated CENPL, SRPX, HELZ2, AFMID, and/or SEC22C antigens and autologous tumor cells. All of the reactive clonotypes were detected at similar levels and appeared in some cases to have increased in the patient's peripheral blood 5 weeks after transfer. In addition, all but one of the tumor-reactive clonotypes were detected at lower but significant levels approximately 1 year after transfer, suggesting an important role of mutation-reactive T cells in the ongoing complete tumor regression observed in some patients receiving adoptive treatment with autologous TILs (7–9).

Overall, these observations suggest that additional clinical studies focused on targeted neoantigens are warranted. Additional treatment strategies that take advantage of whole-exome and RNA-Seq data include the isolation and expansion of T cells specific for patient neoantigens using MHC multimers generated by peptide exchange (38), the transduction of patient PBMCs with TCRs isolated from neoantigen-reactive T cells, and the development of cancer vaccines targeting potent neoantigens. This information can also serve as the basis of therapies combining the checkpoint inhibitors, the adoptive transfer of neoantigen-reactive T cells, and neoantigen vaccines that may result in enhanced therapeutic effects.

Disclosure of Potential Conflicts of Interest

No potential conflicts of interest were disclosed.

References

- Atkins MB, Lotze MT, Dutcher JP, Fisher RI, Weiss G, Margolin K, et al. High-dose recombinant interleukin 2 therapy for patients with metastatic melanoma: analysis of 270 patients treated between 1985 and 1993. *J Clin Oncol* 1999;17:2105–16.
- Rosenberg SA. IL-2: the first effective immunotherapy for human cancer. *J Immunol* 2014;192:5451–8.
- Rosenberg SA, Yang JC, Sherry RM, Kammula US, Hughes MS, Phan GQ, et al. Durable complete responses in heavily pretreated patients with metastatic melanoma using T-cell transfer immunotherapy. *Clin Cancer Res* 2011;17:4550–7.
- Topalian SL, Sznol M, McDermott DF, Kluger HM, Carvajal RD, Sharfman WH, et al. Survival, durable tumor remission, and long-term safety in patients with advanced melanoma receiving nivolumab. *J Clin Oncol* 2014;32:1020–30.
- Rizvi NA, Mazieres J, Planchard D, Stinchcombe TE, Dy GK, Antonia SJ, et al. Activity and safety of nivolumab, an anti-PD-1 immune checkpoint inhibitor, for patients with advanced, refractory squamous non-small-cell lung cancer (CheckMate 063): a phase 2, single-arm trial. *Lancet Oncol* 2015;16:257–65.
- Powles T, Eder JP, Fine GD, Braithel FS, Loriot Y, Cruz C, et al. MPDL3280A (anti-PD-L1) treatment leads to clinical activity in metastatic bladder cancer. *Nature* 2014;515:558–62.
- Robbins PF, Lu YC, El-Gamil M, Li YF, Gross C, Gartner J, et al. Mining exomic sequencing data to identify mutated antigens recognized by adoptively transferred tumor-reactive T cells. *Nat Med* 2013;19:747–52.
- Lu YC, Yao X, Li YF, El-Gamil M, Dudley ME, Yang JC, et al. Mutated PPP1R3B is recognized by T cells used to treat a melanoma patient who experienced a durable complete tumor regression. *J Immunol* 2013;190:6034–42.
- Lu YC, Yao X, Crystal JS, Li YF, El-Gamil M, Gross C, et al. Efficient identification of mutated cancer antigens recognized by T cells associated with durable tumor regressions. *Clin Cancer Res* 2014;20:3401–10.
- Tran E, Turcotte S, Gros A, Robbins PF, Lu YC, Dudley ME, et al. Cancer immunotherapy based on mutation-specific CD4+ T cells in a patient with epithelial cancer. *Science* 2014;344:641–5.
- Snyder A, Makarov V, Merghoub T, Yuan J, Zaretsky JM, Desrichard A, et al. Genetic basis for clinical response to CTLA-4 blockade in melanoma. *N Engl J Med* 2014;371:2189–99.
- Rizvi NA, Hellmann MD, Snyder A, Kvistborg P, Makarov V, Havel JJ, et al. Mutational landscapedetermines sensitivity to PD-1 blockade in non-small cell lung cancer. *Science* 2015;348:124–8.
- Gubin MM, Zhang X, Schuster H, Caron E, Ward JP, Noguchi T, et al. Checkpoint blockade cancer immunotherapy targets tumour-specific mutant antigens. *Nature* 2014;515:577–81.
- Moss DJ, Misko IS, Burrows SR, Burman K, McCarthy R, Sculley TB. Cytotoxic T-cell clones discriminate between A- and B-type Epstein-Barr virus transformants. *Nature* 1988;331:719–21.
- Dudley ME, Wunderlich JR, Shelton TE, Even J, Rosenberg SA. Generation of tumor-infiltrating lymphocyte cultures for use in adoptive transfer therapy for melanoma patients. *J Immunother* 2003;26:332–42.
- Lapointe R, Bellemare-Pelletier A, Housseau F, Thibodeau J, Hwu P. CD40-stimulated B lymphocytes pulsed with tumor antigens are effective antigen-presenting cells that can generate specific T cells. *Cancer Res* 2003;63:2836–43.
- Jones S, Wang TL, Shih Ie M, Mao TL, Nakayama K, Roden R, et al. Frequent mutations of chromatin remodeling gene ARID1A in ovarian clear cell carcinoma. *Science* 2010;330:228–31.
- Pfeifer GP. Formation and processing of UV photoproducts: effects of DNA sequence and chromatin environment. *Photochem Photobiol* 1997;65:270–83.
- Bennett EM, Bennis JR, Yewdell JW, Brodsky FM. Cutting edge: adenovirus E19 has two mechanisms for affecting class I MHC expression. *J Immunol* 1999;162:5049–52.

Authors' Contributions

Conception and design: T.D. Prickett, S.A. Rosenberg, P.F. Robbins
Development of methodology: X. Yao, Y.F. Li, M. El-Gamil, S.A. Rosenberg, P.F. Robbins
Acquisition of data (provided animals, acquired and managed patients, provided facilities, etc.): T.D. Prickett, J.S. Crystal, C.J. Cohen, A. Pasetto, M.R. Parkhurst, X. Yao, Y.F. Li, M. El-Gamil, K. Trebska-McGowan
Analysis and interpretation of data (e.g., statistical analysis, biostatistics, computational analysis): T.D. Prickett, J.S. Crystal, C.J. Cohen, M.R. Parkhurst, J.J. Gartner, X. Yao, R. Wang, M. El-Gamil, K. Trebska-McGowan, S.A. Rosenberg, P.F. Robbins
Writing, review, and/or revision of the manuscript: T.D. Prickett, J.S. Crystal, M.R. Parkhurst, A. Gros, M. El-Gamil, S.A. Rosenberg, P.F. Robbins
Administrative, technical, or material support (i.e., reporting or organizing data, constructing databases): T.D. Prickett, J.S. Crystal, A. Pasetto, A. Gros, M. El-Gamil, K. Trebska-McGowan, S.A. Rosenberg
Study supervision: T.D. Prickett, S.A. Rosenberg, P.F. Robbins
Other (generated tumor cell line from patient studied): A. Gros

Acknowledgments

The authors thank Arnold Mixon and Shawn Farid for their kind assistance with FACS analysis and cell sorting procedures.

Grant Support

This work was supported in part by a grant from the Adelson Medical Research Foundation.

The costs of publication of this article were defrayed in part by the payment of page charges. This article must therefore be hereby marked *advertisement* in accordance with 18 U.S.C. Section 1734 solely to indicate this fact.

Received September 1, 2015; revised April 29, 2016; accepted May 13, 2016; published OnlineFirst June 16, 2016.

20. Ji H, Wang TL, Chen CH, Pai SI, Hung CF, Lin KY, et al. Targeting human papillomavirus type 16 E7 to the endosomal/lysosomal compartment enhances the antitumor immunity of DNA vaccines against murine human papillomavirus type 16 E7-expressing tumors. *Hum Gene Ther* 1999; 10:2727–40.
21. Lundegaard C, Lamberth K, Harndahl M, Buus S, Lund O, Nielsen M. NetMHC-3.0: accurate web accessible predictions of human, mouse and monkey MHC class I affinities for peptides of length 8–11. *Nucleic Acids Res* 2008;36:W509–12.
22. Gros A, Robbins PF, Yao X, Li YF, Turcotte S, Tran E, et al. PD-1 identifies the patient-specific CD8(+) tumor-reactive repertoire infiltrating human tumors. *J Clin Invest* 2014;124:2246–59.
23. Zhou J, Shen X, Huang J, Hodes RJ, Rosenberg SA, Robbins PF. Telomere length of transferred lymphocytes correlates with in vivo persistence and tumor regression in melanoma patients receiving cell transfer therapy. *J Immunol* 2005;175:7046–52.
24. Wolf M, Kuball J, Ho WY, Nguyen H, Manley TJ, Bleakley M, et al. Activation-induced expression of CD137 permits detection, isolation, and expansion of the full repertoire of CD8+ T cells responding to antigen without requiring knowledge of epitope specificities. *Blood* 2007;110: 201–10.
25. Szymczak AL, Workman CJ, Wang Y, Vignali KM, Dilioglou S, Vanin EF, et al. Correction of multi-gene deficiency in vivo using a single 'self-cleaving' 2A peptide-based retroviral vector. *Nat Biotechnol* 2004; 22:589–94.
26. Wargo JA, Robbins PF, Li Y, Zhao Y, El-Gamil M, Caragacianu D, et al. Recognition of NY-ESO-1+ tumor cells by engineered lymphocytes is enhanced by improved vector design and epigenetic modulation of tumor antigen expression. *Cancer Immunol Immunother* 2009;58:383–94.
27. Alexandrov LB, Nik-Zainal S, Wedge DC, Aparicio SA, Behjati S, Biankin AV, et al. Signatures of mutational processes in human cancer. *Nature* 2013;500:415–21.
28. Krauthammer M, Kong Y, Bacchiocchi A, Evans P, Pornputtpong N, Wu C, et al. Exome sequencing identifies recurrent mutations in NF1 and RASopathy genes in sun-exposed melanomas. *Nat Genet* 2015;47:996–1002.
29. Van Allen EM, Miao D, Schilling B, Shukla SA, Blank C, Zimmer L, et al. Genomic correlates of response to CTLA-4 blockade in metastatic melanoma. *Science* 2015;350:207–11.
30. Cohen CJ, Gartner JJ, Horovitz-Fried M, Shamalov K, Trebska-McGowan K, Bliskovsky VV, et al. Isolation of neoantigen-specific T cells from tumor and peripheral lymphocytes. *J Clin Invest* 2015;125:3981–91.
31. Lawrence MS, Stojanov P, Mermel CH, Robinson JT, Garraway LA, Golub TR, et al. Discovery and saturation analysis of cancer genes across 21 tumour types. *Nature* 2014;505:495–501.
32. Johnson LA, Morgan RA, Dudley ME, Cassard L, Yang JC, Hughes MS, et al. Gene therapy with human and mouse T-cell receptors mediates cancer regression and targets normal tissues expressing cognate antigen. *Blood* 2009;114:535–46.
33. Robbins PF, Kassim SH, Tran TL, Crystal JS, Morgan RA, Feldman SA, et al. A pilot trial using lymphocytes genetically engineered with an NY-ESO-1-reactive T-cell receptor: long-term follow-up and correlates with response. *Clin Cancer Res* 2015;21:1019–27.
34. Morgan RA, Chinnsamy N, Abate-Daga D, Gros A, Robbins PF, Zheng Z, et al. Cancer regression and neurological toxicity following anti-MAGE-A3 TCR gene therapy. *J Immunother* 2013;36:133–51.
35. Huang J, El-Gamil M, Dudley ME, Li YF, Rosenberg SA, Robbins PF. T cells associated with tumor regression recognize frameshifted products of the CDKN2A tumor suppressor gene locus and a mutated HLA class I gene product. *J Immunol* 2004;172:6057–64.
36. Zhou J, Dudley ME, Rosenberg SA, Robbins PF. Persistence of multiple tumor-specific T-cell clones is associated with complete tumor regression in a melanoma patient receiving adoptive cell transfer therapy. *J Immunother* 2005;28:53–62.
37. Robbins PF, Dudley ME, Wunderlich J, El-Gamil M, Li YF, Zhou J, et al. Cutting edge: persistence of transferred lymphocyte clonotypes correlates with cancer regression in patients receiving cell transfer therapy. *J Immunol* 2004;173:7125–30.
38. Toebe M, Coccors M, Bins A, Rodenko B, Gomez R, Nieuwkoop NJ, et al. Design and use of conditional MHC class I ligands. *Nat Med* 2006;12:246–51.